Parametric Sensitivities for 2-D Anisotropic Magnetotelluric Models

Josef Pek[1], Fernando A. M. Santos[2] and Yuguo Li[3]

[1]Geophysical Institute, Acad. Sci. Czech Rep., Prague, Czech Republic *

[2]Physics Department–CGUL–University of Lisbon, Portugal

[3]Geophysics Department, Free University of Berlin, Germany

Abstract

Theoretical and numerical principles of the parametric sensitivity calculations for 2-D anisotropic magnetotelluric models are presented. Based on the direct problem formulation and its numerical approximation by the finite volume technique, we derive partial differential equations and boundary conditions for the sensitivities of the magnetotelluric fields with respect to the elements of the conductivity tensor within the medium, as well as with respect to local geometrical parameters of the model. Similarity and symmetry of normal systems of linear equations that result from the finite volume approximation of both the direct and sensitivity problems can be exploited to substantially increase the numerical efficiency of practical sensitivity calculations. For illustration, a simple sensitivity study for a schematic block model is shown.

1 Introduction

Parametric sensitivities play a significant role in geophysical modelling, as they provide quantitative information about the effect that individual structural parameters have on measured data. In a sensitivity analysis, this information can be used to assess the resolution power of a geophysical experiment with respect to specific structures of interest, to estimate the significance of interpreted model parameters, to design the most suitable experimental setup for reliably detecting a specific sub-surface target, etc. Effective algorithms for the sensitivity computations are of primary importance in developing efficient linearized inverse procedures.

This contribution deals with the theory and numerical computations of parametric sensitivities for a specific class of 2-D magnetotelluric (MT) models with arbitrary anisotropy of the electrical conductivity. It is a part, rather technical, of a broader initiative aimed at extending the present direct modelling algorithms for anisotropic media (e.g., Pek and Verner 1997, Li 2002) to a sufficiently automatized inverse procedure for anisotropic conductivities in the earth. Conceptually, the present sensitivity study is based on joining our direct modelling algorithm (Pek and Verner 1997) with well-tried sensitivity evaluation approaches developed earlier for 2-D isotropic models (e.g., Jupp and Vozoff 1977, Pek 1987, Rodi and Mackie 2001).

The structure of the contribution is as follows: In Section 2, we summarize the main features of the 2-D direct MT problem for anisotropic conductors and principles of its solution, both in the theoretical and numerical respect. A few recent algorithmic improvements related to the finite volume (FV) approximation of the problem (Pek and Verner 1997) are pointed out. Section 3 gives a theoretical basis for the sensitivity modelling in 2-D anisotropic MT models and summarizes the principles of the numerical sensitivity computations. Section 4 demonstrates the sensitivity calculations on a simple synthetic block model.

2 2-D Direct MT Problem with Anisotropy

2.1 Model and Basic Equations

The 2-D MT model with arbitrary anisotropy of the electrical conductivity was already analyzed earlier in detail by Reddy and Rankin (1975), Pek and Verner (1997) and Li (2002). Therefore, we will only briefly summarize the principal features of this model and the corresponding numerical algorithm here that are significant for subsequent sensitivity studies.

*e-mail of the corresponding author: jpk@ig.cas.cz

We assume a 2-D electrical model with the axis of homogeneity parallel to the x-coordinate direction. The electrical conductivity of the model is described by a symmetric and positive definite 2-D conductivity tensor $\boldsymbol{\sigma}(y,z)$ for $z>0$ (flat earth model). The air layer above the earth's surface is assumed to be a perfect insulator, i.e., $\sigma \equiv 0$ for $z<0$. The MT field is excited by a uniform and monochromatic electromagnetic plane wave coming from remote sources at $z \to -\infty$ and propagating perpendicularly to the earth's surface. We further assume that (i) the quasi-steady state approximation is applicable to our model, and (ii) the medium considered is non-magnetic, i.e., $\mu \equiv \mu_0$ throughout the whole space, with μ_0 being the vacuum permeability.

By manipulating Maxwell's equations for the particular model characterized above, we easily obtain the basic second order partial differential equations (PDE's) governing the strike-parallel components of the field (e.g., Pek and Verner 1997),

$$\frac{\partial^2 E_x}{\partial y^2}+\frac{\partial^2 E_x}{\partial z^2}+i\omega\mu_0(\sigma_{xx}+S_z\sigma_{xy}+S_y\sigma_{xz})E_x+i\omega\mu_0 S_y\frac{\partial H_x}{\partial y}-i\omega\mu_0 S_z\frac{\partial H_x}{\partial z}=0, \tag{1}$$

$$\frac{\partial}{\partial y}\left(\frac{\sigma_{yy}}{D}\frac{\partial H_x}{\partial y}\right)+\frac{\partial}{\partial z}\left(\frac{\sigma_{zz}}{D}\frac{\partial H_x}{\partial z}\right)+\frac{\partial}{\partial y}\left(\frac{\sigma_{yz}}{D}\frac{\partial H_x}{\partial z}\right)+\frac{\partial}{\partial z}\left(\frac{\sigma_{yz}}{D}\frac{\partial H_x}{\partial y}\right)- \\ -\frac{\partial(S_yE_x)}{\partial y}+\frac{\partial(S_zE_x)}{\partial z}+i\omega\mu_0 H_x=0, \tag{2}$$

where

$$D=\sigma_{yy}\sigma_{zz}-\sigma_{yz}^2, \quad S_y=(\sigma_{yz}\sigma_{yx}-\sigma_{yy}\sigma_{xz})/D, \quad S_z=(\sigma_{xz}\sigma_{yz}-\sigma_{zz}\sigma_{yx})/D.$$

By grouping in (1) and (2) the terms with E_x and H_x together, these equations can be written symbolically,

$$\mathcal{L}^{EE}(E_x)+\mathcal{L}^{EH}(H_x)=0, \tag{3}$$

$$\mathcal{L}^{HE}(E_x)+\mathcal{L}^{HH}(H_x)=0, \tag{4}$$

where $\mathcal{L}^{EE}$, $\mathcal{L}^{EH}$, $\mathcal{L}^{HE}$, $\mathcal{L}^{HH}$ are linear differential operators according to (1), (2).

The mathematical formulation of the model is completed by providing the boundary conditions at infinity as well as at conductivity discontinuities within the conductor. Assuming that the 2-D inhomogeneities are spatially restricted to a finite domain of the model only, the boundary conditions at infinite margins of the model are derived from the respective 1-D solutions for the 1-D conductivity sections $\boldsymbol{\sigma}(\pm\infty,z)$.

The internal boundary conditions link the solutions for E_x, H_x from either side of a boundary at which a jump of the electrical conductivity takes place. In general, the magnetic and tangential electric fields have to be continuous through conductivity discontinuities within the model. For the particular model structure considered here, these general conditions require the following functions to be continuous through the contact,

$$E_x,\ \frac{\partial E_x}{\partial n},\ H_x,\ \frac{1}{D}\left[(\sigma_{yy}n_y+\sigma_{yz}n_z)\frac{\partial H_x}{\partial y}+(\sigma_{yz}n_y+\sigma_{zz}n_z)\frac{\partial H_x}{\partial z}\right]-(S_yn_y-S_zn_z)E_x, \tag{5}$$

where $\mathbf{n}=(0,n_y,n_z)$ is a unit normal vector to the boundary, $n_y^2+n_z^2=1$. For a contact of two isotropic media, the last condition in (5) reduces to the well-known (H-mode) condition of $(\sigma^{-1}\partial H_x/\partial n)$ being continuous through the boundary.

PDE's (1) and (2) and the corresponding boundary conditions define the mathematical model of the 2-D MT direct problem for generally anisotropic media. By solving this problem we obtain the strike-parallel fields E_x and H_x throughout the space. The secondary, transverse field components are then easily computed by using the basic electromagnetic equations,

$$\begin{aligned} H_y&=\frac{1}{i\omega\mu_0}\frac{\partial E_x}{\partial z}, & H_z&=-\frac{1}{i\omega\mu_0}\frac{\partial E_x}{\partial y}, \\ E_y&=\frac{\sigma_{yz}}{D}\frac{\partial H_x}{\partial y}+\frac{\sigma_{zz}}{D}\frac{\partial H_x}{\partial z}+S_zE_x, & E_z&=-\frac{\sigma_{yy}}{D}\frac{\partial H_x}{\partial y}-\frac{\sigma_{yz}}{D}\frac{\partial H_x}{\partial z}+S_yE_x. \end{aligned} \tag{6}$$

2.2 Numerical Approximation by Finite Volume Approach

The 2-D direct MT problem for generally anisotropic conductors has been approximated and solved numerically both by the finite difference (Pek and Verner 1997) and finite element approaches (Reddy and Rankin 1975, Li 2002). In our finite volume (FV) approach to the problem (Pek and Verner 1997), the whole model is first divided into electrically homogeneous rectangular cells by a system of horizontal and vertical lines. Then, a dual

mesh is constructed through the centres of the primary mesh spacing intervals (Fig. 1a), and the integral form of Maxwell's equations is approximated on each of the dual mesh cells by using solely the field values E_x, H_x at the nodes of the primary mesh. By this procedure, we obtain two coupled linear algebraic equations at each mesh node, which correspond to the original PDE's for the quasi-E-mode, eq. (1), and quasi-H-mode, eq. (2). The general form of the FV equations at a (j,k)-th mesh node is

$$\begin{aligned}\sum_{\alpha=j-1}^{j+1}\sum_{\beta=k-1}^{k+1} C^{EE}_{jk,\alpha\beta}E_x(\alpha,\beta) + \sum_{\alpha=j-1}^{j+1}\sum_{\beta=k-1}^{k+1} C^{EH}_{jk,\alpha\beta}H_x(\alpha,\beta) = 0,\\ \sum_{\alpha=j-1}^{j+1}\sum_{\beta=k-1}^{k+1} C^{HE}_{jk,\alpha\beta}E_x(\alpha,\beta) + \sum_{\alpha=j-1}^{j+1}\sum_{\beta=k-1}^{k+1} C^{HH}_{jk,\alpha\beta}H_x(\alpha,\beta) = 0,\end{aligned} \tag{7}$$

where $E_x(\alpha,\beta)$ and $H_x(\alpha,\beta)$ are the fields at the node (α,β), and the coefficients C_{jk} depend both on the conductivities and mesh spacings of the four cells that surround the node (j,k). By their non-zero entries, the two sets of coefficients $C^{EE}_{\alpha\beta}$, $C^{EH}_{\alpha\beta}$ and $C^{HE}_{\alpha\beta}$, $C^{HH}_{\alpha\beta}$, respectively, define two generally 9-point stencils at each mesh node (Fig. 1b).

Fig. 1b shows schematically the situation for the maximum fill-up of the stencils corresponding to the case of four fully anisotropic cells surrounding the central node (j,k). How many of the stencil positions are actually occupied by non-zero values depends on the particular conductivities of the cells involved. In particular, no approximation to the quasi-H-mode equation (2) is done at all on the surface and in the air layer above the conductor, as the air is an isotropic insulator, and the magnetic field $H_x = \text{const}$ on the surface and throughout the air domain. The minimum fill-up of the stencils corresponds to the case of an isotropic model, with the two above quasi-modes decoupled into the standard 2-D E and H field modes.

If a node (α,β) in (7) lies on an external boundary of the model domain, respective boundary conditions are substituted for the fields $E_x(\alpha,\beta)$ and $H_x(\alpha,\beta)$, and the corresponding terms are moved to the r.h.s. of the FV equations. The boundary conditions at $y \to \pm\infty$ are computed by a 1-D field propagation matrix routine (e.g., Reddy and Rankin 1971). To avoid numerical difficulties arising from rapidly increasing exponentials for large wave numbers in the 1-D boundary models, we use a modified version of the standard algorithm for the 1-D field propagation between the top (z_T) and bottom (z_B) of a uniform anisotropic layer, based on combining standard impedance formulas with those for a stable upwards impedance propagation (see, e.g., Dekker and Hastie 1980, Pek and Santos 2002) and stable downwards magnetic field propagation,

$$\begin{pmatrix} H'_x(z_B) \\ H'_y(z_B) \end{pmatrix} = \frac{1}{D_0}\begin{pmatrix} \dfrac{1-\kappa_1 Z'_{xy}(z_B)\tanh k_1 h}{\cosh k_2 h} & -\dfrac{\kappa_2 Z'_{yy}(z_B)\tanh k_2 h}{\cosh k_1 h} \\ \dfrac{\kappa_1 Z'_{xx}(z_B)\tanh k_1 h}{\cosh k_2 h} & \dfrac{1+\kappa_2 Z'_{yx}(z_B)\tanh k_2 h}{\cosh k_1 h} \end{pmatrix}\begin{pmatrix} H'_x(z_T) \\ H'_y(z_T) \end{pmatrix}, \tag{8}$$

$$D_0 = 1 + \kappa_1\kappa_2 \det \mathbf{Z}'(z_B)\tanh k_1 h \tanh k_2 h - \kappa_1 Z'_{xy}(z_B)\tanh k_1 h + \kappa_2 Z'_{yx}(z_B)\tanh k_2 h,$$

$$h = z_B - z_T, \qquad k_j = \sqrt{-i\omega\mu_0\sigma_j}, \quad \kappa_j = k_j/(i\omega\mu_0), \quad j = 1,2,$$

where σ_1, σ_2 are the principal azimuthal conductivities in the layer, and the primed symbols mean components taken in the principal azimuthal conductivity direction.

By ordering the mesh variables E_x, H_x in, e.g., a column-by-column way, the complete set of eqs. (7) throughout the mesh will form a normal system of FV linear algebraic equations,

$$\mathbf{A}\mathbf{u} = \mathbf{b}, \tag{9}$$

where $\mathbf{A}$ is a symmetric and banded matrix of the coefficients C_{jk}, the vector $\mathbf{b}$ is formed of the external boundary conditions of the problem, and $\mathbf{u}$ is a vector of the approximate field values in the mesh nodes. For small and medium size modelling problems, we use the Gaussian direct elimination procedure, slightly modified to benefit from the specific structure of the matrix $\mathbf{A}$, to solve the system (9) (Pek and Verner 1997).

2.3 Secondary Fields and MT Functions

By solving the normal system of FV equations (9), we obtain approximate values of the strike-parallel field components E_x, H_x in all mesh nodes of the FV grid. The secondary field components E_y, E_z, H_y, H_z are then computed by using formulas (6), which requires the spatial derivatives of the primary components E_x, H_x with respect to y and z to be evaluated.

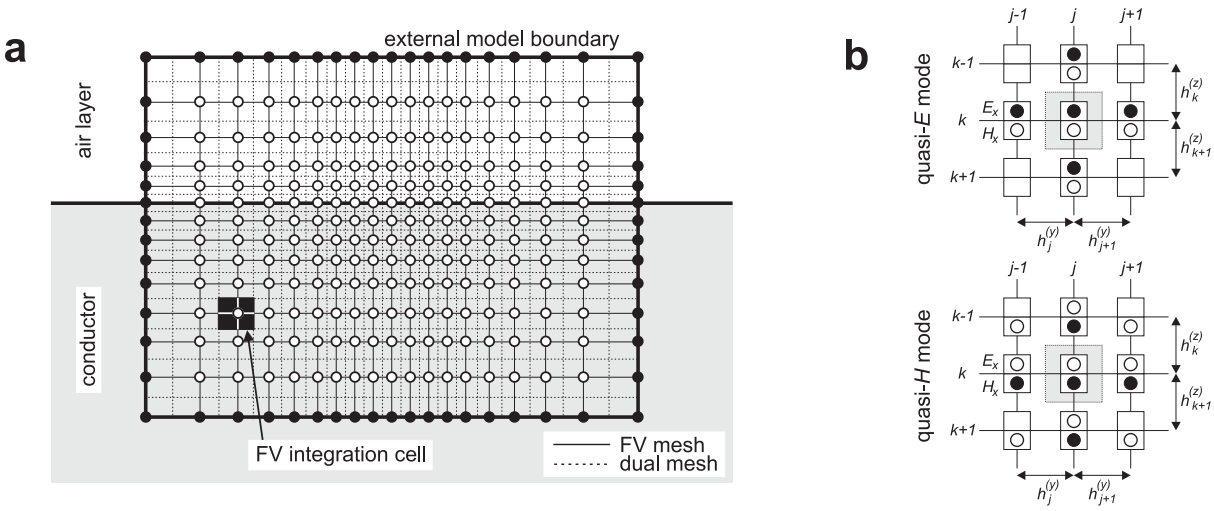

Figure 1: a—Model domain covered by a FV mesh (full lines) and a dual mesh (dashed lines). Empty circles show the internal mesh nodes, full circles are nodes on the extenal boundary of the model domain. One FV integration cell is shown by a black rectangle. b—Schematic stencils arising from FV discretizing eqs. (1) (top) and (2) (bottom). Circles in the top and bottom half-boxes symbolize the presence of a non-zero coefficient with the corresponding field E_x and H_x, respectively, at the given position in the stencil. Full circles show the minimum fill-up of the stencil, corresponding to the isotropic conductor. Empty circles indicate stencil coefficients that arise due to anisotropy.

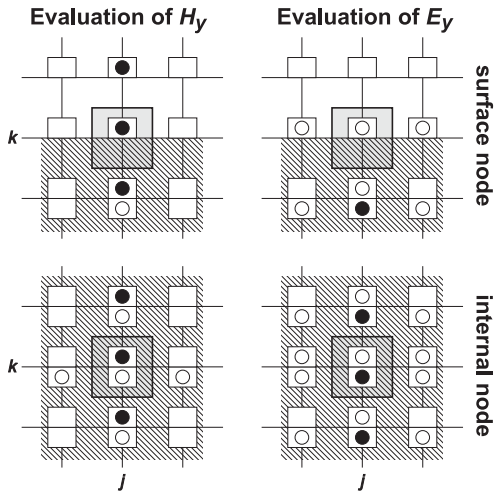

Figure 2: Stencils for the approximation of the transverse field components H_y (left) and E_y (right), showing positions of non-zero coefficients D, eq. (10), around a central node (j, k). The top and bottom panels are for the central node situated on the surface and inside the conductor, respectively. The top and bottom half-boxes at the stencil nodes are for coefficients D^E and D^H, respectively. Full circles show stencil positions occupied in case only a simple parabolic interpolation is used to evaluate the derived fields.

A common way of evaluating the spatial field derivatives numerically at a specific mesh node is to differentiate an interpolating function fitted through a pattern of nodes around the central node. We used, e.g., a three-point central (for E_x) and one-sided (for H_x) parabolic interpolation to approximate the spatial derivatives on the earth's surface in (Pek and Verner 1997). Li (2002) uses a spline interpolation through a whole line of nodes inside the conductor for the same purpose.

Weaver *et al.* (1985, 1986) suggested an improved approach to the numerical evaluation of the spatial derivatives and derived fields in 2-D isotropic models, which more closely conforms the approximation procedure used to solve the underlying direct problem. Pek and Toh (2001) suggested a way how to employ this differentiation procedure within the finite volume approximation context, and could generalize the improved derivative formulas to the case of arbitrarily anisotropic 2-D models. The procedure first performs a suitable conductivity averaging, which modifies the sub-resolution conductivity distribution within each FV integration cell so that (i) the coefficients of the FV equations (7) do not change, and (ii) dealing with inconsistent boundary conditions on sharp boundaries between the individual mesh cells can be avoided. The spatial derivatives of E_x, H_x with respect to y and z can be then easily evaluated by subtracting the FV integrals applied to halves of the standard FV integration cells, with properly averaged conductivities used (Pek and Toh 2001). The resulting secondary fields at a node (j, k) can be then written in a general form,

$$H_y(j,k),\ H_z(j,k),\ E_y(j,k),\ E_z(j,k) \approx \sum_{\alpha=j-1}^{j+1} \sum_{\beta=k-1}^{k+1} \left[D^E_{jk,\alpha\beta} E_x(\alpha,\beta) + D^H_{jk,\alpha\beta} H_x(\alpha,\beta) \right], \qquad (10)$$

with component-specific coefficients D^E, D^H, which can be visualized in a stencil form as shown in Fig. 2 for case of the vertical derivatives.

MT functions, as impedances, geomagnetic transfer functions, etc., can be easily evaluated from the MT field components computed for two different linear polarizations of the primary field (Pek and Verner 1997).

3 Parametric Sensitivities

3.1 Parametric Sensitivities with respect to Subdomain Conductivities

Parametric sensitivities of the approximate direct problem solution $\mathbf{u}$ with respect to a specific parameter p of the medium is defined as a partial derivative $\mathbf{u}^p \equiv \partial\mathbf{u}/\partial p$. A standard way to evaluating $\mathbf{u}^p$ is to directly differentiate the normal system (9) with respect to the parameter p (see, e.g., Vozoff and Jupp 1977),

$$\mathbf{A}\frac{\partial \mathbf{u}}{\partial p} \equiv \mathbf{A}\mathbf{u}^p = -\frac{\partial \mathbf{A}}{\partial p}\mathbf{u} + \frac{\partial \mathbf{b}}{\partial p} \equiv \mathbf{r}_p. \tag{11}$$

The system (11) has the same matrix $\mathbf{A}$ as the original system of the FV equations (9), and the systems differ by their right-hand sides only. The r.h.s. of (11) is easily computed if the direct solution $\mathbf{u}$ and parametric derivatives of the external boundary conditions are known.

If Gaussian elimination is used to solve both the direct and sensitivity systems, (9) and (11), the complete elimination procedure for the matrix $\mathbf{A}$ needs to be carried out only once. Provided the eliminated form of the matrix $\mathbf{A}$ is stored, the solution of (11) involves only a short elimination step for the current r.h.s., $\mathbf{r}_p$, followed by a standard back-substitution (e.g., Jupp and Vozoff 1977, Červ and Pek 1981). This algorithmic modification speeds up the evaluation of the parametric sensitivities substantially.

The above numerical sensitivities $\mathbf{u}^p$ can be shown to exactly correspond to FV approximated field sensitivities $\partial E_x/\partial p$ and $\partial H_x/\partial p$. The partial differential equations that govern these field sensitivities can be derived directly from the basic field equations (1), (2).

Let us assume p to be one of the conductivity tensor elements of a homogeneous domain Π of the model. By varying p to $p + \delta p$ within Π, the strike-parallel MT fields will generally change in the whole model to $E_x + \delta E_x$ and $H_x + \delta H_x$. By successively subtracting the PDE's (1), (2) for the original conductivity p from those written for the modified conductivity distribution $p + \delta p$, dividing the obtained difference by δp, and evaluating a limit for $\delta p \to 0$, we immediately arrive at PDE's for the field sensitivities $E_x^p \equiv \partial E_x/\partial p$, $H_x^p \equiv \partial H_x/\partial p$,

$$\mathcal{L}^{EE}(E_x^p) + \mathcal{L}^{EH}(H_x^p) = -i\omega\mu_0 \frac{\partial(\sigma_{xx} + S_z\sigma_{xy} + S_y\sigma_{xz})}{\partial p} E_x - \\ - i\omega\mu_0 \frac{\partial S_y}{\partial p}\frac{\partial H_x}{\partial y} + i\omega\mu_0 \frac{\partial S_z}{\partial p}\frac{\partial H_x}{\partial z} = 0, \tag{12}$$

$$\mathcal{L}^{HE}(E_x^p) + \mathcal{L}^{HH}(H_x^p) = -\frac{\partial}{\partial y}\left[\frac{\partial}{\partial p}\left(\frac{\sigma_{yy}}{D}\right)\frac{\partial H_x}{\partial y}\right] - \frac{\partial}{\partial z}\left[\frac{\partial}{\partial p}\left(\frac{\sigma_{zz}}{D}\right)\frac{\partial H_x}{\partial z}\right] - \\ - \frac{\partial}{\partial y}\left[\frac{\partial}{\partial p}\left(\frac{\sigma_{yz}}{D}\right)\frac{\partial H_x}{\partial z}\right] - \frac{\partial}{\partial z}\left[\frac{\partial}{\partial p}\left(\frac{\sigma_{yz}}{D}\right)\frac{\partial H_x}{\partial y}\right] + \frac{\partial}{\partial y}\left(\frac{\partial S_y}{\partial p}E_x\right) - \frac{\partial}{\partial z}\left(\frac{\partial S_z}{\partial p}E_x\right), \tag{13}$$

where $\mathcal{L}^{EE}$, $\mathcal{L}^{EH}$ and $\mathcal{L}^{HE}$, $\mathcal{L}^{HH}$ are the linear differential operators introduced by (3), (4). The right-hand sides of (12), (13) are generally non-zero for points in Π only, and they always vanish outside this domain. Consequently, the structure of the field and sensitivity PDE's (3), (4) and (12), (13), respectively, is identical except for the right-hand sides of the latter system within the domain Π.

The differentiation of the field equations with respect to p also affects both the external and internal boundary conditions for the sensitivity problem. The sensitivity conditions on the external boundaries of the model are derived from 1-D sensitivity calculations for the respective 1-D boundary models at $y \to \pm\infty$. In our current algorithm, we combine the derivatives of the standard impedance relations, parametric sensitivites of the impedance tensor according to (Pek and Santos 2002), and derivatives of the magnetic field propagation formula (8) with respect to p, to generate stable external boundary conditions for the 2-D sensitivity problem. Since we do not assume a conductivity variation in a finite domain to affect the fields at infinity, the external sensitivity conditions are always zero for a bounded domain Π.

It can be easily shown that the field sensitivities E_x^p, H_x^p meet the same boundary conditions (5) as the field components themselves through all internal boundaries within the model except the boundary of the domain Π. Through the boundary of Π, only the first three conditions of (5) are valid also for the field sensitivities. The last

one has to be replaced, however, by a more complex boundary condition,

$$\left\{ \frac{1}{D} \left[(\sigma_{yy} n_y + \sigma_{yz} n_z) \frac{\partial H_x^p}{\partial y} + (\sigma_{yz} n_y + \sigma_{zz} n_z) \frac{\partial H_x^p}{\partial z} \right] - (S_y n_y - S_z n_z) E_x^p + \right.$$
$$\left. + \frac{\partial}{\partial p} \left(\frac{\sigma_{yy} n_y + \sigma_{yz} n_z}{D} \right) \frac{\partial H_x}{\partial y} + \frac{\partial}{\partial p} \left(\frac{\sigma_{yz} n_y + \sigma_{zz} n_z}{D} \right) \frac{\partial H_x}{\partial z} - \left(\frac{\partial S_y}{\partial p} n_y - \frac{\partial S_z}{\partial p} n_z \right) E_x \right\}_{\Pi i} =$$
$$= \left\{ \frac{1}{D} \left[(\sigma_{yy} n_y + \sigma_{yz} n_z) \frac{\partial H_x^p}{\partial y} + (\sigma_{yz} n_y + \sigma_{zz} n_z) \frac{\partial H_x^p}{\partial z} \right] - (S_y n_y - S_z n_z) E_x^p \right\}_{\Pi e}, \quad (14)$$

where Πi, Πe symbolize, respectively, the internal and external side of the boundary with respect to Π.

Eqs. (12), (13) with the corresponding boundary conditions can be FV approximated in the same way as the original direct problem (1), (2) in (Pek and Verner 1997). With some more algebra involved, this approximation can be shown to result exactly in the linear system (11). This may be considered a proof of the numerical consistency of the formally introduced differentiation mapping (9)→(11).

System (11) provides $\mathbf{u}^p$ that approximates the parametric sensitivities of the basic fields E_x^p, H_x^p on the numerical mesh. Approximate parametric sensitivities of the derived, transverse fields can be easily obtained by directly differentiating formulas (10) with respect to the parameter p. In virtue of (10), any field component can be expressed at a specific mesh node as $\psi = \mathbf{d}^T \mathbf{u}$, where $\psi \in \{E_x, E_y, E_z, H_x, H_y, H_z\}$ at a (j,k)-th node, and $\mathbf{d}$ consists of the appropriate coefficients D_{jk}^E, D_{jk}^H. Then,

$$\psi^p \equiv \frac{\partial \psi}{\partial p} = \frac{\partial (\mathbf{d}^T \mathbf{u})}{\partial p} = \frac{\partial \mathbf{d}^T}{\partial p} \mathbf{u} + \mathbf{d}^T \mathbf{u}^p = \frac{\partial \mathbf{d}^T}{\partial p} \mathbf{u} + \mathbf{d}^T \mathbf{A}^{-1} \mathbf{r}_p. \quad (15)$$

Parametric sensitivities of an arbitrary MT parameter, which is a function of the field components at one or several mesh nodes, $F = f(\psi_k)$, $\psi_k = \mathbf{d}_k^T \mathbf{u}$, $k = 1, 2, \ldots$, can be obtained by simply using a chain rule,

$$F^p \equiv \frac{\partial F}{\partial p} = \sum_k \frac{\partial F}{\partial \psi_k} \frac{\partial \psi_k}{\partial p} = \sum_k \frac{\partial F}{\partial \psi_k} \frac{\partial \mathbf{d}_k^T}{\partial p} \mathbf{u} + \sum_k \frac{\partial F}{\partial \psi_k} \mathbf{d}_k^T \mathbf{A}^{-1} \mathbf{r}_p. \quad (16)$$

3.2 Evaluating Parametric Sensitivities by Employing the Reciprocity Principle

By solving once the system (11) we obtain the sensitivity $\mathbf{u}^p$ with respect to one particular parameter p throughout the model. For a large number of parameters, such as typical of inverse problems based on the Occam strategy, direct sensitivity evaluations by solving multiple systems (11) are computationally hardly feasible.

The electromagnetic reciprocity principle, declaring interchangeability of field sources and effects, presents a way of substantially reducing the computation time necessary for the sensitivity calculations, provided the number of the mesh nodes at which the sensitivities are to be evaluated is substantially less than the total number of parameters. This results in an acceptable compromise, as in many cases, and for inverse problems in particular, the sensitivities are only required at nodes that correspond to the measurement sites on the earth's surface.

In the numerical domain, the electromagnetic reciprocity principle is expressed by a symmetry of the normal FV matrix $\mathbf{A}$ in (9), i.e., $\mathbf{A} = \mathbf{A}^T$ (e.g., Rodi and Mackie 2001). Then, e.g., (15) can be modified as follows,

$$\psi^p = \frac{\partial \mathbf{d}^T}{\partial p} \mathbf{u} + \mathbf{d}^T \mathbf{A}^{-1} \mathbf{r}_p = \frac{\partial \mathbf{d}^T}{\partial p} \mathbf{u} + \mathbf{d}^T (\mathbf{A}^{-1})^T \mathbf{r}_p = \frac{\partial \mathbf{d}^T}{\partial p} \mathbf{u} + (\mathbf{A}^{-1} \mathbf{d})^T \mathbf{r}_p = \frac{\partial \mathbf{d}^T}{\partial p} \mathbf{u} + \mathbf{g}^T \mathbf{r}_p, \quad (17)$$

where $\mathbf{g}$ solves the system

$$\mathbf{A} \mathbf{g} = \mathbf{d}. \quad (18)$$

Thus, by using (17), ψ^p is computed for *all* parameters p with only once having to solve the system (18) with the appropriate vector $\mathbf{d}$. Altogether, we need four solutions of this system to compute all the sensitivities for all field components relevant to MT studies (E_x, E_y, H_y, H_z, the component H_x is insensitive to any internal parameter) at one node and at one period. Computing the sensitivities for two different polarizations of the exciting field does not add to this number, i.e., again four solutions of (18) are needed to compute all the parametric sensitivities for any standard single-site MT function at one site and one period.

Rodi and Mackie (2001) have shown that further saving is possible if the sensitivity evaluation according to (17) is employed within a non-linear conjugate gradients inverse algorithm, where explicit computations of the sensitivities can be avoided and only products of the sensitivity matrix with a vector are required.

3.3 Parametric Sensitivities with respect to Geometrical Parameters

In models that are products of modern inverse algorithms the geometry is mostly not dealt with explicitly. Boundaries of geological structures are hypothesized from increased conductivity gradients in models that are discretized into a fine mosaic of homogeneous cells. Specific regularization approaches have been suggested to focus large scale structures and sharpen their edges (e.g., Portniaguine and Zhdanov 1999).

Nonetheless, for pure sensitivity studies, it may be sometimes of interest to have a tool for assessing the effect of a varying boundary or depth within the model on MT data. Ku (1976) and Rodi (1976) presented a method that used the grid spacings as geometrical parameters, and computed the geometrical sensitivities in the numerical domain by directly differentiating (9) with respect to the mesh steps. For a properly designed mesh, the sensitivities computed in such a way should be only little affected by the error resulting from the varying mesh geometry. One problem of this approach is that variations in a mesh step can result in geometrical changes in the whole model, and the sensitivity with respect to a particular local geometrical feature may be difficult to distinguish.

Another, more rigourous way to evaluate the geometrical sensitivities is to start from a theoretical formulation of the problem and derive the PDE's and corresponding boundary conditions that control the sensitivity fields. This approach was used by Pek (1987) for 2-D isotropic models.

Let us for simplicity consider a local horizontal boundary section AB (Fig. 3), with its vertical coordinate being z_{AB}. Moving this section by Δz_{AB} into a new position, $A'B'$, causes the MT fields to change throughout the model, from the original value ψ to a perturbed value ψ', where ψ is for any MT component. Now, we define the sensitivity of ψ with respect to $p \equiv z_{AB}$ as follows,

$$\psi^p \equiv \frac{\partial \psi}{\partial z_{AB}} = \lim_{\Delta z_{AB} \to 0} \frac{\psi' - \psi}{\Delta z_{AB}}. \tag{19}$$

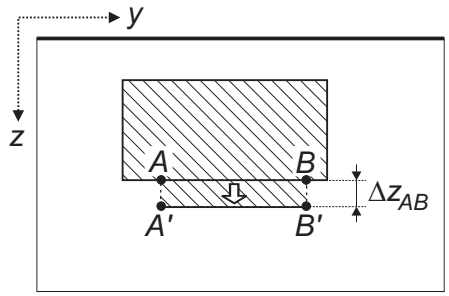

Figure 3: Variation of a local horizontal boundary section AB demonstrating the introduction of the parametric sensitivity with respect to z_{AB} (19).

Considering eqs. (1), (2) for both the unperturbed and perturbed geometry, and by using (19), it can be easily shown that the sensitivities E_x^p, H_x^p are governed by a coupled system of homogeneous PDE's,

$$\mathcal{L}^{EE}(E_x^p) + \mathcal{L}^{EH}(H_x^p) = 0, \tag{20}$$

$$\mathcal{L}^{HE}(E_x^p) + \mathcal{L}^{HH}(H_x^p) = 0, \tag{21}$$

in any domain with a smoothly varying conductivity.

The external boundary conditions for (20), (21) can be obtained from the corresponding 1-D sensitivities with respect to the thicknesses of layers in an anisotropic layered medium (Pek and Santos 2002). Through any internal contact of the medium *except* the section AB itself, the internal boundary conditions (5) can be shown to be valid also for E_x^p and H_x^p. Deriving the boundary conditions through AB requires a special treatment as described in (Pek 1987). Without going further into detail here, we can prove that the following functions are continuous through the horizontal boundary section AB,

$$\begin{aligned} &E_x^p, && \frac{\partial E_x^p}{\partial z} - i\omega\mu_0 \left[(\sigma_{xx} + S_z\sigma_{xy} + S_y\sigma_{xz})E_x + S_y \frac{\partial H_x}{\partial y} - S_z \frac{\partial H_x}{\partial z} \right], \\ &H_x^p + \frac{\partial H_x}{\partial z}, && \frac{\sigma_{zz}}{D}\frac{\partial H_x^p}{\partial z} + \frac{\sigma_{yz}}{D}\frac{\partial H_x^p}{\partial y} + S_z E_x^p + \frac{\partial}{\partial y}\left(\frac{\sigma_{yy}}{D}\frac{\partial H_x}{\partial y} + \frac{\sigma_{yz}}{D}\frac{\partial H_x}{\partial z} - S_y E_x \right). \end{aligned} \tag{22}$$

In contrast to the field boundary conditions (5), the boundary conditions for the geometric sensitivities E_x^p, H_x^p are more complex. Only E_x^p is continuous through a contact, H_x^p and the normal derivatives of both E_x^p and H_x^p are discontinuous, with jumps depending both on the conductivity contrasts through the boundary and on the behaviour of the direct solution E_x, H_x near the boundary section AB. The boundary conditions (22) can be easily modified for a vertical boundary section, and, after some generalization to the sensitivity definition, for an oblique contact as well.

PDE's (20), (21) along with the corresponding external boundary conditions and conditions (22) through internal contacts represent a complete system which can be solved for the sensitivities of the MT field with respect to the coordinate of the local boundary section AB. FV approximation of this system is rather straightforward and results in a linear algebraic system analogous to (11). Special attention has to be paid, however, to the approximation steps with the discontinuous boundary conditions (22) involved.

4 Numerical Example

The parametric sensitivity analysis for anisotropic models has been primarily considered an auxiliary tool within a broader study aimed at developing an inversion algorithm for 2-D anisotropic MT structures, which would also be the main application scope of the present study. Here, for illustration purposes, we present only a very simple 2-D model analysis to demonstrate the sensitivity calculations. The model chosen consists of a homogeneous resistive halfspace with the resistivity of 1000 Ωm and a conductive anomalous block with the resistivity of 1 Ωm, size of 10×1.5 km, situated at the depth of 9 km below the surface (Fig. 4a). The question to be analyzed by the sensitivity studies is how the surface MT functions of this model respond to small *unidirectional* variations of the conductivity within that part of the host medium that overlies the anomaly (hatched in Fig. 4a). First, we analyze the effect of a horizontal conductivity variation of the host on the geomagnetic transfer functions W_x and W_y, defined by $H_z = W_x H_x + W_y H_y$. For the original (isotropic!) model, the strike-parallel component $W_x = 0$. Real and imaginary parts of W_y are shown in Fig. 4b.

Panels Fig. 4c through 4f display the sensitivities of W_x, W_y with respect to the principal horizontal resistivity ϱ_1 of the layer above the conductive block for different principal directions $\alpha_S \in (0, 90)$ deg. Clearly, the largest effect on W_y, but no effect at all on W_x, is observed if the resistivity changes along the strike, i.e., for $\alpha_S = 0$ deg. Resistivity variations in the transverse direction, i.e., for $\alpha_S = 90$ deg, do not show any influence on the geomagnetic transfer functions, since only H-mode fields are affected in this case. Except for these two

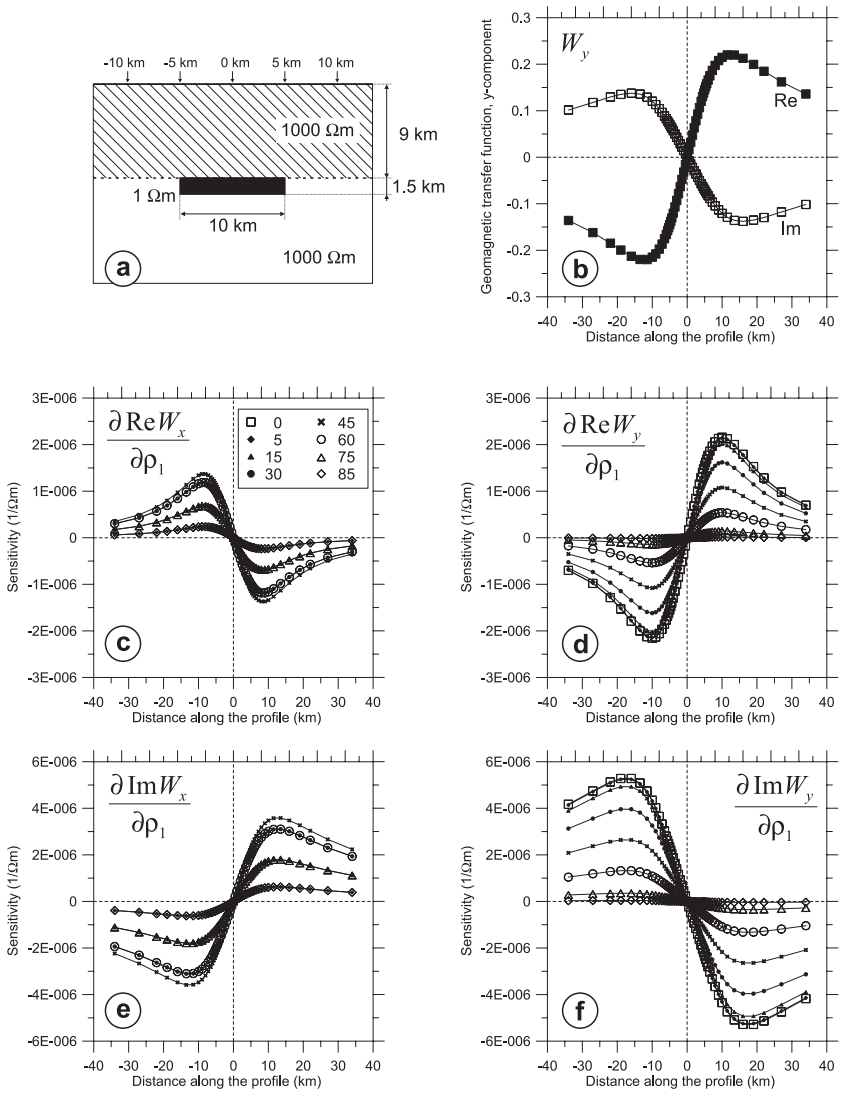

Figure 4: Sensitivities of the geomagnetic transfer functions with respect to the principal resistivities of the host medium. a—Model of a conducting anomaly in a resistive host. The sensitivities are computed with respect to the principal resistivities of the hatched layer. b—Real and imaginary parts of the geomagnetic transfer function W_y on the surface. c, d, e, f—Sensitivities of W_x, W_y with respect to a horizontal principal resistivity ϱ_1 in various directions $\alpha_S \in (0, 90)$ deg. The curve symbols for the specific values of α_S are shown in the legend to panel c.

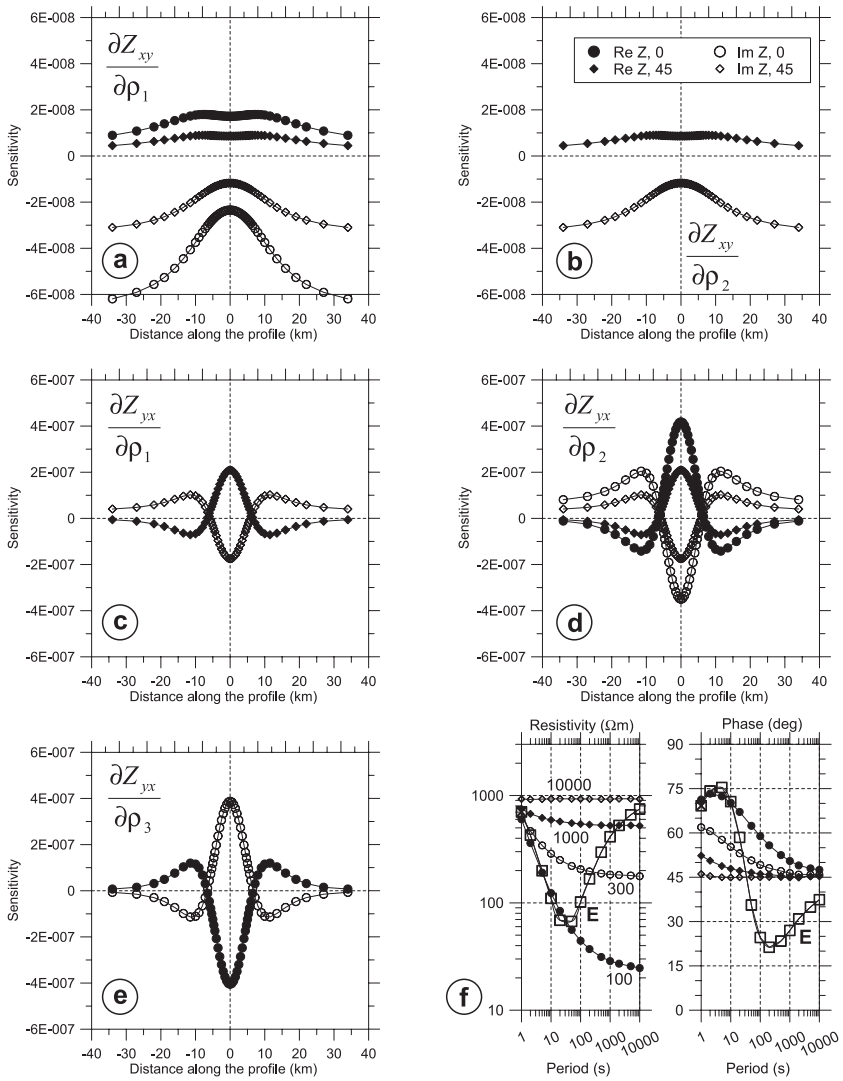

Figure 5: Sensitivities of the off-diagonal MT impedances with respect to the principal resistivities of the host medium for the model from Fig. 4a. a, b—Sensitivities of Z_{xy} with respect to the horizontal principal resistivities ϱ_1 ($\parallel \alpha_S$) and ϱ_2 ($\perp \alpha_S$) for two values of the azimuth, $\alpha_S = 0$ and 45 deg. c, d—The same as in a, b, but for the impedance element Z_{yx}. Missing curves for $\alpha_S = 0$ would correspond to sensitivities equal to zero. e—Sensitivity of Z_{yx} with respect to the vertical principal resistivity ϱ_3. f—Comparison of resistivity and phase curves above the center of the model for various values of the vertical resistivity $\varrho_3 \in (100, 10000)$ Ωm. E is the E-mode curve, which does not depend on the vertical resistivity, the other curves correspond to the H-mode and are labeled according to ϱ_3 in Ωm.

marginal cases, the mode coupling generally causes both W_x and W_y to respond to the principal resistivity variations. In terms of conductivity variations, $\sigma_1 = 1/\varrho_1$, increasing the conductivity σ_1 in a general direction α_S, $0 < \alpha_S < 90$, results in a decrease of $\mathrm{Re}\, W_y$ and a positive $\mathrm{Re}\, W_x$ arising along the positive section of the profile, $y > 0$, and vice versa along its negative section. This agrees with a phenomenon described earlier by Schmucker (1994) and Pek and Verner (1997) that, in structures similar to our model, the real induction arrows, $T_R = (\mathrm{Re}\, W_x, \mathrm{Re}\, W_y)$, do not strictly obey the rule of perpendicularity to the strike, but, quite the contrary, are attracted *towards* the direction of the best conductivity within the anisotropic layer. The imaginary parts of the geomagnetic transfer functions show similar behaviour (Fig. 4d, f).

Another example analyzes, for the same model setting as above, the sensitivity of MT parameters with respect to a variation in the vertical principal resistivity $\varrho_3 \equiv \varrho_z$ within the top layer of the model. This parameter is often disregarded in MT studies as it is known to be absolutely 'invisible' in 1-D layered MT models.

Fig. 5 shows the sensitivities of the off-diagonal impedance elements Z_{xy}, Z_{yx} both with respect to the principal horizontal resistivities, ϱ_1 and ϱ_2, and to the vertical resistivity, ϱ_3, for two directions of the variation azimuths, $\alpha_S = 0$ and 45 deg. Clearly, for $\alpha_S = 0$ deg, Z_{xy} and Z_{yx} do not sense ϱ_2 ($\perp \alpha_S$) and ϱ_1 ($\parallel \alpha_S$), respectively. As any change in the vertical resistivity leaves the E and H-field modes uncoupled in our specific model, variation in ϱ_3 can be sensed by the impedance component Z_{yx} only. Panels c, d, e in Fig. 5 show that this sensitivity, measured by $\partial Z_{yx}/\partial \varrho_3$, is far from neglible, and is quite comparable to the sensitivities of Z_{yx} with respect to

the horizontal resistivity variations. A serious effect of the vertical resistivity on MT data is further illustrated by Fig. 5f that shows the apparent resistivities and phases above the center of our model for different vertical resistivities $\varrho_3 \in (100, 10000)\ \Omega$m.

5 Conclusion

Parametric sensitivities provide serious information for assessing the significance and resolvability of the structural parameters of the model under study, and are an indispensable part of linearized inverse algorithms. In this contribution, we have tried to present a comprehensive description of both the theoretical and numerical aspects of the sensitivity computations for a specific class of 2-D MT models with arbitrary anisotropy of the electrical conductivity. Starting from the direct problem formulation (3), (4), (5), and its numerical FV approximation (9), we could derive theoretical formulations of and numerical approximations to the parametric sensitivity problems for both the physical and geometrical parameters, i.e., for conductivity tensor elements, eqs. (12), (13), (14), and (11), and for local boundary sections, eqs. (20), (21), (22). In numerical respect, all the advantages of the normal matrix $\mathbf{A}$ being symmetric and common to both the direct and sensitivity problems could be easily exploited in the anisotropic case as well.

Further research aimed at incorporating the MT sensitivity computation algorithm into a linearized inversion for 2-D anisotropic conductivities is going on.

Acknowledgements

This study has been financially supported by the Grant Agency of the Academy of Sciences of the Czech Republic through the grant No. A3012401, as well as by the Ministry of Education, Youth and Sports of the Czech Republic through the contract KONTAKT ME 677. Two of the authors, J.P. and F.A.M.S., would like to thank the Academy of Sciences of the Czech Republic and the GRICES Portugal for their support given to the Czech-Portuguese cooperation within the project 'Magnetotelluric Interpretation of Electrically Anisotropic Earth's Structures'.

References

Červ, V. and Pek, J., 1981. Numerical solution of the two-dimensional inverse geomagnetic induction problem, *Stud. geophys. geod.*, **25**, 69–80.

Dekker, D. L. and Hastie, L. M., 1980. Magnetotelluric impedances of an anisotropic layered Earth model, *Geophys. J. R. astr. Soc.*, **61**, 11–20.

Jupp, D. L. B. and Vozoff, K., 1977. Two-dimensional magnetotelluric inversion, *Geophys. J. R. astr. Soc.*, **50**, 333–352.

Ku, C. C., 1976. Numerical inverse magnetotelluric problem, *Geophysics*, **41**, 276–286.

Li, Y., 2002. A finite-element algorithm for electromagnetic induction in two-dimensional anisotropic conductivity structures, *Geophys. J. Int.*, **148**, 389–401.

Pek, J., 1987. Numerical inversion of 2D MT data by models with variable geometry, *Phys. Earth Planet. Int.*, **45**, 193–203.

Pek, J. and Santos, F. A. M., 2002. Magnetotelluric impedances and parametric sensitivities for 1-D anisotropic layered media, *Computers & Geosciences*, **28**, 939–950.

Pek, J. and Toh, H., 2001. Numerical modelling of MT fields in 2-D anisotropic structures with topography and bathymetry considered, in *Proc. 18th Colloq. "Electromagnetic Depth Investigations", Altenberg, March 20–24, 2000*, Hoerdt, A. and Stoll, J. (Eds.), DGG, pp. 190–199.

Pek, J. and Verner, T., 1997. Finite-difference modelling of magnetotelluric fields in two-dimensional anisotropic media, *Geophys. J. Int.*, **128**, 505–521.

Portniaguine, O. and Zhdanov, M. S., 1999. Focusing geophysical inversion images, *Geophysics*, **64**, 874–887.

Reddy, I. K. and Rankin, D., 1971. Magnetotelluric effect of dipping anisotropies, *Geophysical Prospecting*, **19**, 84–97.

Reddy, I. K. and Rankin, D., 1975. Magnetotelluric response of laterally inhomogeneous and anisotropic media, *Geophysics*, **40**, 1035–1045.

Rodi, W. L., 1976. A technique for improving the accuracy of finite element solutions for MT data, *Geophys. J. R. astr. Soc.*, **44**, 483–506.

Rodi, W. and Mackie, R. L., 2001. Nonlinear conjugate gradients algorithm for 2-D magnetotelluric inversion, *Geophysics*, **66**, 174–187.

Schmucker, U., 1994. 2D Modellrechnungen zur Induktion in inhomogenen dünnen Deckschichten über anisotropen geschichteten Halbräumen, in *Proc. 15th Colloq. "Electromagnetic Depth Investigations", Höchst in Odenwald, March 28–31, 1994*, Bahr, K. and Junge, A. (Eds.), pp. 3–26.

Weaver, J. T., Le Quang, V. B. and Fischer, G., 1985. A comparison of analytical and numerical results for a two-dimensional control model in electromagnetic induction—I. B-polarization calculations, *Geophys. J. R. astr. Soc.*, **82**, 263–278.

Weaver, J. T., Le Quang, V. B. and Fischer, G., 1986. A comparison of analytical and numerical results for a 2-D control model in electromagnetic induction—I. E-polarization calculations, *Geophys. J. R. astr. Soc.*, **87**, 917–948.